Distributed and Secure Uplink Power Control in Dynamic Spectrum Access

Yousi Lin[®], Yaling Yang, Member, IEEE, Xiaojiang Du, Fellow, IEEE, and Jie Wu[®], Fellow, IEEE

Abstract—In dynamic spectrum access (DSA), secondary users (SU) should only be allowed to access a licensed band belonging to incumbent users (IU) when the quality-of-service (QoS) requirements of both IUs and SUs can be satisfied at the same time. However, IU's location and its received interference strength are considered sensitive in many DSA systems which should not be revealed, making it very challenging to optimize the network utility subjected to satisfying the operation and security requirements of SUs and IUs. In this paper, we develop a secure and distributed SU transmit power control algorithm to solve this challenge. Our algorithm achieves optimal SU power control to maximize the sum of SU rates. The SINR-guaranteed coexistence between SUs and IUs are enabled to maintain effective communication, while no information is directly required from IUs. Local measurements of IU signals provided by Environmental sensing capability (ESC) also undergo a security masking process to ensure that IU location cannot be derived from its outputs. Convergence and stability properties of our algorithm and its privacy-protection strength are both theoretically analyzed and experimentally evaluated through simulations.

Index Terms—DSA, distributed power control, network utility optimization.

I. INTRODUCTION

as a promising solution to mitigate the spectrum scarcity problem caused by the rapid growth in the demand for wireless communication. The key form of the DSA recommended by NTIA [1] and FCC [2] is to share the licensed bands belonging to government incumbents with commercial wireless devices. DSA systems deployed in 3.5 GHz band is one of the eminent DSA architectures. This architecture is composed of a spectrum access system (SAS) and an ESC system [3]. ESC system is a distributed network of sensors built to detect the IU's presence in 3.5 GHz band and inform SAS with its received signal strength (RSS) of IU signals. SAS is responsible for

Manuscript received 20 June 2021; revised 4 December 2021; accepted 4 June 2022. Date of publication 21 June 2022; date of current version 12 December 2022. This work was supported by the National Science Foundation under Grant 1824494. The associate editor coordinating the review of this article and approving it for publication was W. Zhang. (Corresponding author: Yousi Lin.)

Yousi Lin and Yaling Yang are with the Department of Electrical and Computer Engineering, Virginia Tech, Blacksburg, VA 24061 USA (e-mail: yousil94@vt.edu; yyang8@vt.edu).

Xiaojiang Du is with the Department of Electrical and Computer Engineering, Stevens Institute of Technology, Hoboken, NJ 07030 USA.

Jie Wu is with the Department of Computer and Information Sciences, Temple University, Philadelphia, PA 19122 USA.

Color versions of one or more figures in this article are available at https://doi.org/10.1109/TWC.2022.3183078.

Digital Object Identifier 10.1109/TWC.2022.3183078

granting and coordinating SUs' access to the spectrum based on the reported activities of both IUs and SUs. Specifically, SUs are not allowed to access the licensed channel unless it can be concluded from ESC-provided IU sensing results that no harmful interference to the IUs will be triggered by SUs' transmission. Power control for secondary networks, thus, can be a feasible way to ensure an SU can obtain such transmission permission to coexist with IUs. In this paper, we mainly focus on the uplink SU power control in 3.5 GHz DSA systems aiming at maximizing secondary network utility.

One crucial challenge of designing optimal power control schemes for the above DSA system is that some IU information (e.g. IU location information) required in making an optimal power allocation is sensitive and cannot be revealed to any other user. Essentially, when making an optimal power assignments, all SUs need to be jointly coordinated to optimize the network utility, which traditionally requires a centralized controller with global knowledge of the entire network. However, centralized optimal power allocation is not feasible considering IU privacy protection and the inevitably heavy computational overheads on the controller. A practical scheme, thus, has to be decentralized without requiring any sensitive information exchange between users.

Several existing works attempt to partially address the optimal SU power control problem, and we will discuss them in three categories: centralized optimization algorithms, distributed algorithms for SUs only and distributed algorithms for all tiers of users. Centralized optimization algorithms, such as those proposed in [4], [5], lack scalability when the number of SUs in the system is large because the central controller has to coordinate all SUs and becomes the bottleneck. In addition, the central controller needs to know sensitive IU operation data, violating IU's privacy protection demand. Distributed SU power control strategies, such as [6], [7], solves the scalability issues, but is even worse in IU privacy protection since they have to distribute sensitive IU location and interference level information to all SUs. Distributed power control algorithms for all tiers of users, such as [8], [9], do not share the IU's information with SUs, but they assume that all users (including both SUs and IUs) will participate in the power adaptation procedure simultaneously. Such assumption is also not feasible in 3.5 GHz DSA since IU operations in this band are independent to SU operations and classified.

To fill in the void of existing works, in this paper, we formulate the uplink power control problem in DSA scenarios as a utility maximization problem, which is then solved using a proposed distributed and secure algorithm. The key idea of the

1536-1276 © 2022 IEEE. Personal use is permitted, but republication/redistribution requires IEEE permission. See https://www.ieee.org/publications/rights/index.html for more information.

algorithm is that each SU can distributively adapt its transmit power to maximize the sum of throughput while satisfying the IU's interference requirements and preserving the IU's location privacy. We theoretically prove the uplink power control algorithm's convergence at the maximum of network utility, and also show that both IU's interference constraint and SU's power limit and SINR requirement are satisfied at the optimal stable point whenever the formulated problem is feasible. When the optimization problem is infeasible, our algorithm can still converge to a sub-optimal point where all requirements are satisfied except some SU's SINR constraints. In this case, SINR of SUs is sacrificed due to IU's interference protection or SU's power limit. This is reasonable because in DSA, FCC regulation demands that IU's performance has to be guaranteed and SU's maximum power limit cannot be exceeded. Furthermore, no exchange of sensitive IU operation information is required in the algorithms. Instead of directly sharing the raw IU signal strength sensed by ESC, we proposed a geometry-based model so that the algorithm only requires some ESC processed values related to IU signal strength. Our algorithm ensures that accurate operation information of IU cannot be derived from the masked information exchanged in this system.

The remainder of this paper is organized as follows. Section III reviews the related works. Section III introduces the system model and formulates the uplink power control problem in the DSA system. Section IV provides a brief introduction on D.C. programming as a preliminary to our algorithm. Section V describes how each SU uses our algorithm to distributively adjust its transmit power, and the convergence and stability properties of the uplink algorithm are demonstrated in Section VI. Section VII further shows how IU's interference requirement is statistically guaranteed based on geometry modeling. Section VIII analyzes that even when the ESC-supplied information is leaked, it is still difficult for adversaries to infer the true IU location. Evaluations are provided in Section IX. Finally, Section X concludes this paper.

II. RELATED WORK

A. Transmit Power Control for SUs

In [10], [11], several global optimization algorithms are proposed to achieve the optimal network utility. These algorithms either offer some theoretical and mathematical solutions such as convex relaxation and branch-and-bound methods to the target optimization problem, or provide some centralized strategies with a central controller to manage the transmit power of all SUs within its coverage. The theoretical solutions provide no indication on the implementation, and the centralized algorithms have to deal with the heavy communication cost as the number of SU increases. Also, SU and IU privacy is a concern in centralized power control because the central controller need to know the location information and operation states of SUs and IUs.

Second group of approaches [6], [7] focus on distributed SU power control strategies, where SUs distributively adapt the transmit power based on some optimal formulation

with target objective and constraints. Only locally observable measurements and received information are used. However, these schemes provide no privacy protection on IU's information. Many of them assumed that IU's location is known to all SUs and hence each SU can locally measure the channel gain between IU and itself. Some even need to put a genie near an IU to obtain the interference level at the IU's location. Thus, these algorithms will not be compatible with the strict IU operation privacy protection requirement in 3.5GHz DSA system.

Algorithms in [8], [9] distributively adjust the transmit power of different tiers of users simultaneously to achieve maximum utility. They developed the cognitive radio network duality which decouples the transmit power, SINR assignment and the interference threshold allocation. IU's location information is assumed unknown to SU in their algorithms. However, the assumption that IUs will coordinate with SUs to adapt their transmit powers is also not feasible in 3.5 GHz DSA since IU operations in this band should be independent to SU operations.

All of the above schemes require IUs to either reveal their private information or actively join the power adaptation in secondary networks to ensure their received interference will not exceed an allowable threshold. In this paper, we successfully avoid the above problems and provide a privacy-protecting distributed power control algorithm for SUs. In our designs, ESC does not provide any information directly related to an IU's location to SAS, so that no high-overhead encryption is needed to ensure IU privacy in the SU power allocation process. In Section VIII, we formally demonstrate that under our design, it is difficult for an adversary (e.g., malicious SAS or SUs) to accurately infer the IU's location using ESC-provided information.

B. Location Privacy Protection for IUs

IU location privacy protection in DSA has attracted much attention recently. These schemes can be mainly divided into three categories. The first category [12], [13] protects IU's operational information using anonymity, clustering or pertubation based methods. In second category [3], [14], IU's location information is concealed by adding noise, distortion or other blind factor on its inputs to SAS. Works in the third category [15], [16] recruit homomorphic encryption based techniques where IUs' inputs are encrypted before being sent to SAS. However, all these approached assume IU's participation in spectrum sharing process and require modification of IU designs, hence cannot be applied off-theshelf to many DSA systems. Another work [17] do not demand IU's participation in spectrum sharing process. It encrypts the ESC's input to SAS with a proxy re-encryption scheme, which requires a central trusted Key Issuer for keys distribution to SUs and ESCs. How an IU can trust such a Key Issuer remains unclear. Furthermore, the heavy encryption schemes lead to high communication overhead, where the cost of communication is in the magnitude of hundreds of MB and the handling time per SU operation permission reaches thousands of seconds. Hence, these existing schemes for IU location

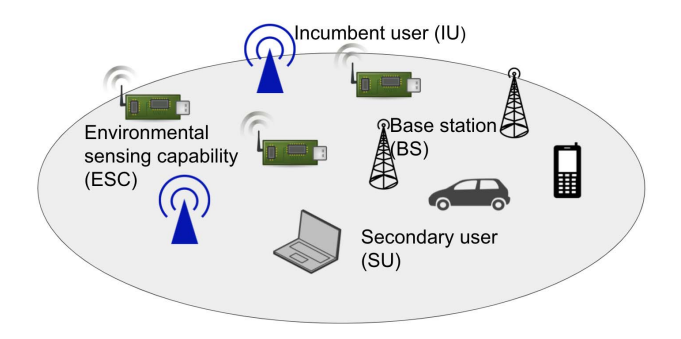


Fig. 1. System model.

privacy protection cannot be directly applied to solve the problem of secure uplink transmit power control in DSA.

III. PROBLEM FORMULATION

The system model considered in the paper is illustrated in Figure 1. Specifically, we assume that m_1 IUs, m_2 ESC sensors, and n pairs of SUs and BSs are distributed in an area. Both the IUs and SUs can be mobile. In uplink, all SUs transmit on the same frequency band. We assume an SU i ($i \in [1, n]$) only transmits towards a BS i. Note that a BS that receives messages from multiple SUs can be modeled as multiple co-located BSs, each communicating with one SU.

One typical objective of an uplink power control problem is to find the optimal power allocation that maximizes the sum of individual rates in uplink. To formulate the problem, denote the transmit power of SU i as P_i . The path attenuation from SU i to BS j is denoted by g_{ij} . The SINR of SU i received at BS i, thus, can be expressed by $SINR_i = \frac{P_i g_{ii}}{\sum_{j \neq i} P_j g_{ji} + \varphi_i}$, where $P_i g_{ii}$ denotes the SU i's signal strength detected at BS i, $\sum_{j \neq i} P_j g_{ji}$ denotes the BS i's received interference from all other SU js $(j \neq i)$, and φ_i denotes the environmental noise between SU i and BS i including the additive receiver noise.

Since the QoS requirements of IU and SUs need to be satisfied, the uplink power control problem can be formulated as:

$$\max_{\mathbf{P}} \sum_{i=1}^{n} log_{2}(\frac{P_{i}g_{ii}}{\sum_{j\neq i} P_{j}g_{ji} + \varphi_{i}} + 1)$$

$$s.t. \frac{P_{i}g_{ii}}{\sum_{j\neq i} P_{j}g_{ji} + \varphi_{i}} \ge \tau, i \in [1, n]$$
(1a)

$$Pr(\sum g_{iI}P_i \le T) \ge \Lambda$$
 (1b)

$$0 \le P_i \le P_{max}, i \in [1, n]$$
 (1c)

The objective is to maximize the sum of SU rates. τ denotes the minimum required SINR level for SU to maintain effective communications as shown by constraint (1a). Note that the constraints in (1a) are actually the linear constraints. Constraint (1b) shows the IU's interference requirement. g_{iI} represents the signal attenuation from SU i to the IU, and T denotes the IU's interference tolerance threshold. Constraint (1b) in essence states that the probability that the

aggregated SU interference received at IU is no larger than the IU's interference requirement T must be no smaller than an acceptable threshold Λ . Constraint (1c) shows that SUs' transmit power P_i is not allowed to exceed its maximum P_{max} .

Though the constraints in problem (1) are straightforward, it is hard to guarantee them directly. Due to IU's location privacy protection, g_{iI} in problem (1) should not be revealed to any SU/BS/ESC. Thus, neither the direct measurement nor the theoretical estimate of interference suffered by IU is feasible. In addition, an IU in 3.5GHz band usually does not have real-time communications with any SU/BS/ESC. Thus, it is also impossible to expect IU to inform SU about its local interference level.

Our solution is to translate the constraints on IU's received interference to the restrictions on ESC's received interference, which can then be directly measured or theoretically estimated by ESC since ESCs' location information can be found publicly according to FCC regulation in 3.5GHz [18]. Specifically, we propose that once an ESC e has detected the existence of IU, it uses the sensing results of IU to derive its local requirement on the maximum allowable SU interference, denoted as T_e . The computation of T_e demonstrates that the aggregated SU signals at IU is likely to be constrained below T if every ESC's received interference from SUs does not exceed T_e (See Section VII for details). Thus, the formulation in (1) is converted into (2):

$$\max_{\mathbf{P}} \sum_{i=1}^{n} log_2 \left(\frac{P_i g_{ii}}{\sum_{j \neq i} P_j g_{ji} + \varphi_i} + 1 \right)$$
 (2)

s.t. (1a), (1c)

$$\sum_{i} P_{i} g_{ie} \le T_{e}, e \in [i, m_{2}]$$
(2b)

where g_{ie} is the signal attenuation from SU i to ESC e. It can be seen that direct IU location information is not required for SU utility maximization in this formulation (2).

Denote the SU power assignments that solve the optimization problem in formulation (2) as a solution set S := $\{P|P \text{ solves } (2)\}, \text{ where } P \text{ is a column vector and } P =$ $\{P_i, i \in [1, n]\}$. In the following sections, we will present our distributed uplink power control algorithm and analyze the convergence and stability of our algorithm. When the solution set S exists, meaning that all three constraints can be satisfied together, our algorithm successfully converges at the optimal stable point in S. When a solution to (2) does not exist (a.k.a. $S = \emptyset$), meaning that a power setting satisfying all three constraints in (2) does not exist, our algorithm will converge to a sub-optimal point that guarantees IU's QoS requirement (2b) and SU's upper power limit constraint (1c), while SUs' SINR constraints (1a) may be violated. We believe this to be a desirable feature of our algorithm because in DSA system, guarantee of IU's QoS is generally a strict requirement, while degrading SU communication quality is often acceptable when the system becomes too crowded with SUs.

IV. D.C. PROGRAMMING

The uplink power control problem in (2) has a non-convex objective, and thus can be hard to solve. Fortunately, D.C.

programming is extensively developed to cover almost all non-convex global optimization problems. Among the general D.C. approaches, DCA is a robust and efficient method to solve large-scale DC programs [10]. Based on DC programming, rewrite (2) as:

$$\max_{\mathbf{P}} h_1(\mathbf{P}) - h_2(\mathbf{P}) \quad s.t. \ (1a), (1c), (2b)$$
 (3)

$$h_1(\mathbf{P}) = \sum_{i=1}^n log_2(\sum_j P_j g_{ji} + \varphi_i)$$
 and $h_2(\mathbf{P}) = \sum_{i=1}^n log_2(\sum_{j\neq i} P_j g_{ji} + \varphi_i)$ are both concave.

As presented in [10], DCA iteratively locates the global optimal solution of (3) by generating a sequence $\{\bar{\mathbf{P}}^{(t)}, t = 0, 1, 2, \ldots\}$ of improved feasible solutions. Specifically, initialized from a feasible starting point $\bar{\mathbf{P}}^{(0)}$, $\bar{\mathbf{P}}^{(t+1)}$ is computed as the optimal solution to the t-th convex sub-problem, which is formulated as:

$$\max_{\mathbf{P}} h_1(\mathbf{P}) - h_2(\bar{\mathbf{P}}^{(t)}) - \nabla h_2(\bar{\mathbf{P}}^{(t)})^{\top} (\mathbf{P} - \bar{\mathbf{P}}^{(t)})$$
s.t. $(1a), (1c), (2b)$ (4)

where $\nabla h_2(\bar{P}_i^{(t)})$ is the gradient of $h_2(\bar{\mathbf{P}}^{(t)})$ at each $\bar{P}_i^{(t)}$, as expressed as:

$$\nabla h_2(\bar{P}_i^{(t)}) = \frac{1}{\ln 2} \sum_{j \neq i} \frac{g_{ij}}{\sum_{k \neq j} \bar{P}_k^{(t)} g_{kj} + \varphi_j}$$
 (5)

Since (4) is convex, whenever the global optimal solution $\bar{\mathbf{P}}^{(t+1)}$ to (4) exists, it must be unique.

Also, it has been proved in [10] that the sequence $\{\bar{\mathbf{P}}^{(t)}, t=0,1,2,\ldots\}$ of improved solutions always converges in finite iterations. The iterative process can be terminated at $|\bar{\mathbf{P}}^{(t)} - \bar{\mathbf{P}}^{(t-1)}| \leq \epsilon_0$ or $|\sum_i \bar{P_i}^{(t)} g_{ij} - \sum_i \bar{P_i}^{(t-1)} g_{ij}| \leq \epsilon_0$, where $\epsilon_0 > 0$ is some threshold. Note that DCA is designed only based on its local characteristics, it cannot theoretically guarantee the globality of converged solutions for general DC programs. However, in practice, DCA converges quite often to a global solution, and is proved to be more robust and more efficient than related standard methods [19], [20]. In Section IX, we compare the performance of DCA and a global optimizer, which shows that DCA indeed performs better in our case.

Essentially, the procedure of DCA can be regarded as a nested loop. The inner loops are responsible for computing each $\bar{\mathbf{P}}^{(t)}$ as the solution to every (t-1)-th convex subproblem (4) to form the sequence of improved solutions $\{\bar{\mathbf{P}}^{(t)}, t=0,1,2,\ldots\}$, so that the outer loop (envelope) can approach the optimal solution to the original non-convex problem (3) (i.e., problem (2)) based on the sequence $\{\bar{\mathbf{P}}^{(t)}, t =$ $\{0,1,2,\ldots\}$. DCA provides a theoretical idea to find the global optimum of D.C. problems efficiently. However, it cannot be directly applied to the scenario of uplink power control in 3.5 GHz DSA systems, because it does not have any indication on a practical way to solve the sub-problems (4) in such scenario. In our proposed SU transmit power control algorithm, presented in the following sections, we adopt the general idea of DCA and demonstrate that our algorithm can solve the sub-problem (4) in a practical and distributed manner repeatedly to generate the sequence of improved solutions, and thus the optimal solution to original problem (2) can be approached iteratively and distributively.

TABLE I
OUR DISTRIBUTED UPLINK POWER CONTROL ALGORITHM

V. OUR DISTRIBUTED UPLINK POWER CONTROL ALGORITHM

In this section, we present our distributed uplink power control algorithm. The key idea of the algorithm is that each SU adjusts its transmit power in a distributed way to maximize the total throughput as well as to meet its SINR requirement and IU's interference requirement, without using or leaking the sensitive IU location information. In the algorithm, SUs only require some IU-insensitive information from BSs and do not need to communicate with other SUs. To achieve this, we adopt the general concept of DCA in our algorithm design.

As discussed, the procedure of DCA is a nested loop. Thus, our algorithm also contains an outer loop and several inner loops. Similar to DCA, our algorithm will generate the sequence of improved solutions $\{\bar{\mathbf{P}}^{(t)}, t = 0, 1, 2, \ldots\}$ which construct the envelope, and each element $\bar{\mathbf{P}}^{(t)}$ inside the sequence is essentially the converged SU transmit power of each (t-1)-th inner loop and is also the initial transmit power of t-th inner loop. In our algorithm, the solution $\bar{\mathbf{P}}^{(t)}$ to every convex sub-problem (4) will be distributively computed, and hence the optimal power allocation of original problem (2) can also be gradually approached in a distributed way. The algorithm can be divided into four parts: the ESC update algorithm, the SAS update algorithm, the BS update algorithm, and the SU update algorithm. The procedure of our algorithm is presented in Table I, and the details of each part and each parameter will be described in the following.

A. ESC Update Algorithm

As in Table I, each ESC e measures its local aggregated SU interference, denoted as C_e , and then updates SAS in every iteration inside each inner loop with

$$\Delta_e = (\eta_2 T_e - C_e) \eta_1, \tag{6}$$

Here, η_1 and η_2 are two random numbers in the range of (0,1]. Both η_1 and η_2 take different values for each Δ_e computation to increase the variations in the value of Δ_e to ensure privacy-protection of IU. The detailed analysis for IU location protection can be found in Section VIII. T_e is the

maximum allowable interference at ESC e. ESC e generates T_e based on its local RSS of IU and the IU's maximum acceptable interference level T posted by the IU. In Section VII, we will discuss the details of T_e generation.

In the ESC update algorithm, we assumes ESC to be able to differentiate IU signals from SU signals based on the dissimilarities in their signal characteristics (e.g. modulation schemes). Such signal classification can be realized through many existing approaches [21]–[23]. Most of current and proposed ESC design proposals already have this capability.

B. SAS Update Algorithm

SAS calculates the minimum value of ESC-supplied Δ_e s, denoted by Δ , which is computed by $\Delta = \min(\Delta_e, e \in [1, m_2])$, and then forwards Δ to all BSs in every iteration within each inner loop.

C. BS Update Algorithm

As in Table I, at every t-th point of the outer loop, BS j broadcasts a parameter $\Gamma_j^{(t)}$ which is the sum of its received SU interference and environmental noise level. While in each iteration of the inner loops, BS j broadcasts a set of parameters including Δ , $f_i'\lambda_i^2$ and Ω_j for each associated SU i. We will explain the details of each parameter in the following.

In the inner loops, the BS's parameter f'_i for its associated SU i is computed as follows:

$$f_i' := f'(\tau - SINR_i) = \begin{cases} 1, & SINR_i < \tau \\ 0, & SINR_i > \tau \end{cases}$$
 (7)

where
$$f(z) := \max(0, z)$$
. (8)

In addition, for each associated SU i, λ_i is a non-zero positive time dependent variable that is updated by the following differential equation:

$$\dot{\lambda}_i = \frac{d\lambda_i}{dt} = \beta_i f(\tau - SINR_i) 2\lambda_i. \tag{9}$$

where β_i is a positive number. β_i is designed to always guarantee $\lambda_i \leq \lambda_{max}$, where λ_{max} is a very large number. β_i is updated by ensuring:

$$\lambda_{i} + \dot{\lambda}_{i} = \lambda_{i} + \beta_{i} f(\tau - SINR_{i}) 2\lambda_{i} \leq \lambda_{max}$$

$$\Rightarrow 0 < \beta_{i} \leq \frac{\lambda_{max} - \lambda_{i}}{2\lambda_{i} f(\tau - SINR_{i})}$$
(10)

Note that the initial $\lambda_i(0)$ must be positive and satisfy $\lambda_i(0) \ll \lambda_{max}$ to ensure λ_i and β_i to be non-negative. And it is easy to achieve because $\lambda_i(0)$ can be determined by BS itself.

In the inner loops, BS j also computes its total received signal and noise strength, denoted as Ω_j , which is the sum of its received signal level and environmental noise level. BS j then broadcasts Ω_j in every iteration of every inner loop.

Thus, each BS j broadcasts the parameter $\Gamma_j^{(t)}$ at the each t-th point of the outer loop, and it also broadcasts the global parameters Δ , Ω_j , $f_i'\lambda_i^2$ for $i \in [1,n]$ to its associated SUs in every iteration within each inner loop. The update frequency and information exchange rate between BS j and its associated SUs is evaluated in Section IX.

D. The SU Update Algorithm

SU i adapts its transmit power P_i in every iteration inside each inner loop by:

$$\dot{P}_{i} = \alpha_{i} \chi_{i}, \qquad (11)$$

$$\chi_{i} = \left[\sum_{k} \frac{g_{ik}}{\Omega_{k}} - \sum_{k \neq i} \frac{g_{ik}}{\Gamma_{k}^{(t)}} - f_{i}' \lambda_{i}^{2} g_{ii} + \sum_{k \neq i} f_{k}' \lambda_{k}^{2} \tau g_{ik}\right] P_{i}, \qquad (12)$$

$$\alpha_i \le \Delta \left| \frac{1}{n_{V_i a_{is}}} \right|. \tag{13}$$

In the above algorithm, Δ , Ω_j , $f_i'\lambda_i^2$ $(i,j\in[1,n])$ are broadcasted by BSs at every iteration of each inner loop, while $\Gamma_i^{(t)}$ is broadcasted by BSs at each outer loop iteration and remains the same during the entire inner loop. Channel gain g_{ik} from SU i to BS k can be measured by SU i using downlink reference (e.g. beacon signal). For example, in time-division duplex (TDD) systems, BSs will broadcast beacon signals at a fixed reference power once or twice within each frame. Due to channel reciprocity in TDD systems, SUs can measure its uplink channel gain to various BSs based on these downlink reference signals [24], [25]. SU i can estimate its channel gain g_{ie} to each ESC e using radio propagation model based on the ESC's location, which is public information. α_i is a locally computed step size based on a step size control function described in Section VI-C. The step size value depends on both locally observable and measurable parameters g_{ie} and χ_i , and a global scalar parameter Δ from BS's broadcasts.

In our algorithm, only locally observable and measurable information and some insensitive aggregated information broadcasted by BSs are required for each SU to update its transmit power distributively. The broadcasted information from BSs reveals no IU location or IU interference levels. Also, accurate IU location or interference level cannot be derived using the information transmitted from ESC to BS. The computation in BS side is not difficult and requires no privacy sensitive information from IU. In Section VI, we prove that our system will asymptotically converge into an optimal stable point in the set S whenever S is nonempty. Then, we will demonstrate how the system stabilizes when S is empty.

VI. CONVERGENCE AND STABILITY OF OUR UPLINK POWER CONTROL ALGORITHM

In this section, we prove the convergence of our uplink power control algorithm. Note that theoretically, the aggregated SU interference at ESC e can be expressed as $C_e = \sum_i P_i g_{ie}$, the total received signal and noise strength Ω_j at BS j can be written as $\Omega_j = \sum_k P_k g_{kj} + \varphi_j$, and the received SU interference and noise level $\Gamma_j^{(t)}$ at BS j is expressed as $\Gamma_j^{(t)} = \sum_{k \neq j} \bar{P}_k^{(t)} g_{kj} + \varphi_j$. The value of $\Gamma_j^{(t)}$ will not change during inner loop iterations.

Combining this with (9) and (11), power update algorithm at SU i can be re-expressed as:

$$\dot{P}_i = \alpha_i [\widetilde{\dot{P}}_i - f_i' \lambda_i^2 g_{ii} + \sum_{k \neq i} f_k' \lambda_k^2 \tau g_{ik}] P_i, \tag{14}$$

where
$$\widetilde{P}_{i} = \sum_{j} \frac{g_{ij}}{\sum_{k} P_{k} g_{kj} + \varphi_{j}}$$

$$- \sum_{j \neq i} \frac{g_{ij}}{\sum_{k \neq j} \overline{P}_{k}^{(t)} g_{kj} + \varphi_{j}}, \qquad (15)$$

$$\dot{\lambda}_i = \beta_i f \left[-(P_i g_{ii} - \tau (\sum_{k \neq i} P_k g_{ki} + \varphi_i)) \right] 2\lambda_i.$$
 (16)

Since f(z) in (7) is not differentiable at z=0, we only consider the convergence of the algorithm in the domain where $P_ig_{ii} > \tau(\sum_{k\neq i} P_kg_{ki} + \varphi_i), i \in [1,n]$ to ensure the existence of f'_i over $[0,P_{max}]$. Essentially, in this section, we will examine the system's convergence to an uplink transmit power allocation set \widetilde{S} that is defined as $\widetilde{S} := \{\mathbf{P} | \mathbf{P} \text{ solves } (17)\}$:

$$\max_{\mathbf{P}} \sum_{i=1}^{n} log_2 \left(\frac{P_i g_{ii}}{\sum_{k \neq i} P_k g_{ki} + \varphi_i} + 1 \right)$$
 (17)

s.t.
$$\frac{P_i g_{ii}}{\sum_{k \neq i} P_k g_{ki} + \varphi_i} > \tau, i \in [1, n]$$
 (17a)
 $(1c), (2b)$

Comparing \widetilde{S} to the solution set S to problem (2), we have $\widetilde{S} \subset S$. Thus, once the system converges into \widetilde{S} , it also converges into S and solve problem (2). We will prove that whenever \widetilde{S} is nonempty, our algorithm will stabilize at it and hence maximizes the sum of SU rates in uplink as well as satisfies both IU and SUs' requirements. Even when an optimal solution does not exist (i.e. $\widetilde{S} = \emptyset$, all three constraints cannot be guaranteed together), the system will asymptotically converge to a sub-optimal stable point which always satisfies SU's maximum power constraint (1c) and the ESC's interference constraint (2b).

As mentioned, our algorithm should converge to an optimal solution $\bar{\mathbf{P}}^{(t+1)}$ of the convex sub-problem (4) during the inner loop inside the t-th iteration of the outer loop, such that the improved sequence $\{\bar{\mathbf{P}}^{(t)}, t=0,1,2,\ldots\}$ is gradually generated, and the optimal power allocation of problem (17) can be asymptotically approached. Note that the constraints of problem (17)'s corresponding convex sub-problem are also (17a), (1c) and (2b). Our proof includes four stages and a special case. We only consider the case where (17) is feasible (i.e., \widetilde{S} is not empty) in the four stages. Convergence in the special case where $\widetilde{S}=\emptyset$ is analyzed in Section VI-E.

For $\widetilde{S} \neq \emptyset$, in stage 1, we first consider a simplified optimization problem by removing SU's SINR constraint (17a), its upper power limit (1c) and ESC's interference constraint (2b) in sub-problem (4). Through the relaxed problem, we derive the first condition that an optimal power allocation must satisfy to maximize the objective of (4). In the next stage, constraint (17a) is reconsidered. We prove the system's convergence at a point satisfying both the optimal condition derived in stage 1 and the constraint (17a). In stage 3, a step size control method is proposed to guarantee ESC's interference constraint (2b). In stage 4, we show how SU's maximum power constraint (1c) is guaranteed with a simple stop criterion. Since IU's interference constraint should be treated with higher priority than SU's SINR requirement, we prove that by using this algorithm, IU's requirement is

satisfied in any cases even when SUs' and IUs' requirements cannot be satisfied simultaneously (i.e. $\widetilde{S} = \emptyset$).

A. Stage 1: A Relaxed Problem

To derive the first condition for the optimal solution of convex sub-problem (4), let's consider a simplified problem by removing SU's constraints (17a) and (1c) and ESC's interference constraint (2b). The problem now becomes:

$$\max_{\mathbf{P}} h_1(\mathbf{P}) - h_2(\bar{\mathbf{P}}^{(t)}) - \nabla h_2(\bar{\mathbf{P}}^{(t)})^{\top} (\mathbf{P} - \bar{\mathbf{P}}^{(t)})$$
where $h_1(\mathbf{P}) = \sum_{i=1}^n log_2(\sum_j P_j g_{ji} + \varphi_i),$

$$h_2(\bar{\mathbf{P}}^{(t)}) = \sum_{i=1}^n log_2(\sum_{i \neq i} P_j^{(t)} g_{ji} + \varphi_i). \tag{18}$$

Since it is a convex problem, the unique optimal solution to (18) is given by:

$$\frac{1}{\ln 2} \sum_{j} \frac{g_{ij}}{\sum_{k} P_{k} g_{kj} + \varphi_{j}} - \nabla h_{2}(\bar{P}_{i}^{(t)}) = 0, \quad i \in [1, n]$$
(19)

Essentially, the optimal power allocation solution for (17) must satisfy (19), meaning that the equilibrium of our power control algorithm must first satisfy (19).

B. Stage 2: Proof of System Convergence at a Point Satisfying (19) and (17a)

In this subsection, we consider SU's SINR constraint (17a). We prove that the system will stabilize at a unique point satisfying both the optimal condition (19) and constraint (17a), such that the objective in (4) is maximized and SUs' SINR requirements are guaranteed.

For ease of notation, denote the power setting meeting the optimal condition (19) and SUs' SINR constraint (17a) as a column vector $\widetilde{Z} := \{ \mathbf{P} | \mathbf{P} \text{ satisfies (19) and (17a)} \}.$

Theorem 1: Starting from any initial state $0 < P_i(0) < P_{max}$, the system described in (14) to (16) asymptotically converges to an optimal power allocation setting \widetilde{Z} .

Proof: The proof includes two steps. At step 1, we prove that the power setting \widetilde{Z} is a saddle point of our algorithm. At step 2, by constructing a Lyapunov function, we prove that the system is asymptotically stable at \widetilde{Z} .

Step 1: Denote $P^* = \{P_i^*, i \in [1, n]\}, \lambda^* = \{\lambda_i^*, i \in [1, n]\}$ as the saddle point of the system. Setting $\dot{P}_i = 0$ and $\dot{\lambda}_i = 0, i \in [i, n], P^*$ is defined by:

$$\begin{cases} \dot{P}_{i} = \alpha_{i} [\tilde{\dot{P}}_{i} - f_{i}' \lambda_{i}^{2} g_{ii} + \sum_{k \neq i} f_{k}' \lambda_{k}^{2} \tau g_{ik}] P_{i}^{*} = 0 & (20a) \\ \tilde{\dot{P}}_{i} = \sum_{j} \frac{g_{ij}}{\sum_{k} P_{k}^{*} g_{kj} + \varphi_{j}} & (20b) \\ - \sum_{j \neq i} \frac{g_{ij}}{\sum_{k \neq j} \bar{P}_{k}^{(t)} g_{kj} + \varphi_{j}} & (20b) \\ \dot{\lambda}_{i} = f[-(P_{i}^{*} g_{ii} - \tau(\sum_{k \neq i} P_{k}^{*} g_{ki} + \varphi_{i}))] 2\lambda_{i} = 0 & (20c) \end{cases}$$

Since $\lambda_i>0$, from (20), it is clear that $f[-(P_i^*g_{ii}-\tau(\sum_{k\neq i}P_k^*g_{ki}+\varphi_i))]=0$, which, based on $f(\cdot)$ definition in (7), means $\frac{P_i^*g_{ii}}{\sum_{k\neq i}P_k^*g_{ki}+\varphi_i}>\tau$. Hence, $f_i'=0, \forall i\in[i,n]$, and $\dot{P}_i=0$ becomes equivalent to $\tilde{P}_i=0$. Thus, (20) to (20) can be converted to:

$$\begin{cases}
\sum_{j} \frac{g_{ij}}{\sum_{k} P_{k}^{*} g_{kj} + \varphi_{j}} = \sum_{j \neq i} \frac{g_{ij}}{\sum_{k \neq j} \bar{P}_{k}^{(t)} g_{kj} + \varphi_{j}}, \\
\frac{P_{i}^{*} g_{ii}}{\sum_{k \neq i} P_{k}^{*} g_{ki} + \varphi_{i}} > \tau, \forall i \in [1, n]
\end{cases}$$
(21)

Based on (5) and (19), clearly (21) is equivalent to the definition of \widetilde{Z} . Hence, \widetilde{Z} equals the saddle point P^* for the system.

Step 2: Given the system's saddle point \widetilde{Z} , now we prove that \widetilde{Z} is the equilibrium of the system and the system converges at \widetilde{Z} by constructing a Lyapunov function $K(\lambda, P)$ as

$$K(\boldsymbol{\lambda}, \boldsymbol{P}) := V(\boldsymbol{\lambda}, \boldsymbol{P}) + F(\boldsymbol{\lambda}, \boldsymbol{P}),$$
where $V := \sum_{j} \ln(\sum_{k} P_{k} g_{kj} + \varphi_{j}) - \sum_{j} \nabla h_{2}(\bar{P}_{j}^{(t)}) P_{j} \ln 2,$

$$F := \sum_{j} f[\tau(\sum_{k \neq j} P_{k} g_{kj} + \varphi_{j}) - P_{j} g_{jj}] \lambda_{j}^{2}.$$
(22)

Theorem 2: $K(\lambda, \mathbf{P})$ defined in (22) is a Lyapunov function for the system defined in (14) - (16). In addition, K = 0 if and only if $\mathbf{P}^* = \widetilde{Z}$.

Proof: The partial derivative of $V(\lambda, P)$ in (22) over P_i is derived as:

$$\frac{\partial V}{\partial P_i} = \sum_{j} \frac{g_{ij}}{\sum_{k} P_k g_{kj} + \varphi_j} - \sum_{j \neq i} \frac{g_{ij}}{\sum_{k \neq j} \bar{P_k}^{(t)} g_{kj} + \varphi_j}$$
$$= \tilde{P_i}$$
(23)

Similarly, the partial derivative of $F(\lambda, \mathbf{P})$ in (22) over P_i and λ_i are derived as:

$$\frac{\partial F}{\partial P_i} = -f_i' \lambda_i^2 g_{ii} + \sum_{k \neq i} f_k' \lambda_k^2 \tau g_{ik}, \tag{24}$$

$$\frac{\partial F}{\partial \lambda_i} = f[\tau(\sum_{k \neq i} P_k g_{ki} + \varphi_i)) - P_i g_{ii}] 2\lambda_i = \dot{\lambda_i} / \beta_i \quad (25)$$

Then we prove that $K(\cdot)$ is a Lyapunov function for the system described by (14) - (16). Since we are discussing a maximization problem, the convergence condition are $\dot{K} \geq 0$ and $K(\cdot)$ is upper bounded, and $\dot{K}=0$ if and only if $\mathbf{P}^*=\widetilde{Z}$.

Firstly, we show that $K(\cdot)$ is upper bounded. The function $K(\cdot)$'s second order partial derivative over P_i satisfies $\frac{\partial^2 K}{\partial P_i^2} < 0$, thus, $K(\cdot)$ is concave over P_i . From (10) we can see that $\lambda_i \leq \lambda_{max}$ is always true. Thus, $K(\cdot)$ is also upper bounded over λ_i .

Next, the time derivative of $K(\cdot)$ is computed by $\dot{K} = \sum_{i} \frac{\partial K}{\partial P_{i}} \dot{P}_{i} + \sum_{i} \frac{\partial K}{\partial \lambda_{i}} \dot{\lambda}_{i}$. Based on (24), the value of $\sum_{i} \frac{\partial K}{\partial \lambda_{i}} \dot{\lambda}_{i}$ can be calculated as $\sum_{i} \frac{\partial K}{\partial \lambda_{i}} \dot{\lambda}_{i} = \sum_{i} \dot{\lambda}_{i}^{2} / \beta_{i} \geq 0$, and

 $\begin{array}{l} \sum_{i}\frac{\partial K}{\partial\lambda_{i}}\dot{\lambda_{i}}=0 \ \ \text{if and only if} \ \ \frac{P_{i}g_{ii}}{\sum_{k\neq i}P_{k}g_{ki}+\varphi_{i}}>\tau, i\in[1,n]. \\ \text{In this case,} \ f'_{i}=0, i\in[1,n]. \\ \text{Next step is to compute} \ \sum_{i}\frac{\partial K}{\partial P_{i}}\dot{P}_{i}. \ \ \text{Given (14), (15), (23)} \end{array}$

Next step is to compute $\sum_i \frac{\partial K}{\partial P_i} P_i$. Given (14), (15), (23) and (24), $\sum_i \frac{\partial K}{\partial P_i} \dot{P}_i = \sum_i (\frac{\partial V}{\partial P_i} + \frac{\partial F}{\partial P_i}) \dot{P}_i = \sum_i \frac{1}{\alpha_i P_i} \dot{P}_i^2 \geq 0$. Hence, $\sum_i \frac{\partial K}{\partial P_i} \dot{P}_i = 0$ if and only if $\dot{P}_i = 0$. Since $f_i' = 0$, $P^* = \tilde{Z}$. $K(\cdot)$ is proved to be a Lyapunov function of our system.

C. Stage 3: Step Size Control for IU's Interference Constraint

So far we only consider the constraints (17a) in problem (17). In this section, ESC's interference constraint (2b) is taken into account. We show that IU's interference requirement (ESC's interference constraint) can be guaranteed in any case by proposing a step size control method.

The step size control method need to ensure that the ESC's interference at any iteration to be smaller than its threshold T_e by enforcing $\sum_{i \in [1,n]} (P_i + \dot{P}_i) g_{ie} \leq T_e, e \in [1,m_2]$. In this way the requirement $\sum_i P_i^* g_{ie} \leq T_e$ can be guaranteed. Since $C_e = \sum_i P_i g_{ie}$, given (11), we can have:

$$\sum_{i} \dot{P}_{i} g_{ie} = \sum_{i} \alpha_{i} \chi_{i} g_{ie} \le \sum_{i} \alpha_{i} |\chi_{i}| g_{ie} \le T_{e} - C_{e}$$
 (26)

Since $T_e - C_e \ge \Delta_e \ge \Delta$, (26) must hold if the following inequality $\sum_i \alpha_i |\chi_i| g_{ie} \le \Delta$ is satisfied: Thus, our algorithm limits α_i , $\forall i \in [1,n]$ setting by $\alpha_i \le \Delta |\frac{1}{n\chi_i g_{ie}}|$.

Essentially, each SU i tunes the step size α_i in each iteration based on the above inequality, which ensures the ESC's interference requirements will not be exceeded at any time.

D. Stage 4: Stopping Criterion

Finally, we handle the maximum power constraint (1c) of SUs. There are cases when the transmit power P_i of SU i already reaches P_{max} , while the optimal solution has not been achieved. In this case, SU i will simply stop increasing its P_i and keep $P_i = P_{max}$ unless the algorithm guides it to decrease the transmit power, while other SUs keep on updating their transmit power until the convergence of the system. Now, we have proved that our algorithm will asymptotically converge to the optimal solution $\bar{\mathbf{P}}^{(t+1)}$ of sub-problem (4) through the inner loop at every t-th outer loop iteration. Hence, the optimal power allocation of problem (17) can be gradually approached based on the constructed sequence $\{\bar{\mathbf{P}}^{(t)}, t=0,1,2,\ldots\}$ of improved solutions.

E. Special Case: $\widetilde{S} = \emptyset$

There are cases where all three constraints in (17) cannot be guaranteed together (i.e., $\widetilde{S}=\emptyset$). In such a case, our algorithm chooses a rational step size based on Stage 3 to ensure at least IU' interference requirement is always satisfied. Moreover, the stopping criterion is applied to guarantee that SU's transmit power is within the allowable range. Note that in this case, the algorithm sacrifices the SINR of SUs. Thus, the constraint (2a) may be violated. This is reasonable because in DSA, FCC regulation demands that IU's performance has

to be guaranteed and SU's maximum power limit cannot be exceeded. Therefore, in this special case, some SUs have to fix their transmit power due to ESC's interference requirement or SU's transmit power limit unless the algorithm guides them to update the transmit power, while other SUs keep on updating their transmit power until the convergence of the system.

VII. ESC INTERFERENCE REQUIREMENTS

As discussed in Section III, due to the sensitivity in IU's location privacy, the interference from SUs to an IU cannot be directly measured and thus the uplink problem formulation in (1) cannot be solved directly. Therefore, we estimate the interference from SU to ESC instead and create problem formulation (2). In Section VI, we have proved that our uplink power control algorithm asymptotically stabilize at an equilibrium that solves the respective optimization problems with ESCs' requirements. In this section, we describe how our algorithm computes ESC's interference constraint T_e and verify that using this T_e computation, the solution to the uplink problem in (2) is approximately also a solution to (1).

From a high level, denoting T_E as the set of all T_e , T_E can be computed by solving:

$$U(\mathbf{T_E}) := Pr(I \le T | C_e \le T_e, \text{ for all } e \in [1, m_2]) \ge \Psi$$
(27)

where Ψ is a constant threshold satisfying $\Psi \in [0,1]$ and $\Psi \approx 1$. We denote the left side of the inequality as $U(\mathbf{T_E})$, which represents the conditional probability that the aggregated SU interference I at IU does not exceed its requirement T given that the SU interference C_e received at each ESC e is bounded by $\mathbf{T_E}$. The formula essentially means that ESCs should choose a proper $\mathbf{T_E}$ to ensure the probability on the left side to be close to 1.

In the next sections, we derive the explicit expression of $U(\mathbf{T_E})$. To achieve this, we first present the geometric model of our system in Section VII-A. Based on the model, we derive the statistical distribution of C_e in Section VII-B. In Section VII-C, we model the statistical distribution of I. Next, in Section VII-D, (27) is solved as a cumulative density function (CDF) of a conditional normal distribution, and use this CDF to determine T_E that guarantees $U(\mathbf{T_E}) \geq \Psi$.

A. Geometry-Based Heterogeneous Network Modeling

The network architecture used in our model is shown in Figure 2. Here we consider a heterogeneous network containing different tiers of SUs. The IU is denoted by green triangle. In this section, we take one IU case as an example for detailed explanation. The case of multiple IUs is discussed in Section VII-E. All SUs are denoted by red crosses. SUs inside each orange area form a cluster, and are regarded as the hotspot SUs. The average number of hotspot SUs per cluster is n_s . The center of clusters, denoted by blue dots, are modeled as a homogeneous Poisson Point Process (PPP) with the density of ρ_1 . Hotspot SUs are distributed around cluster centers according to a Gaussian distribution (a.k.a. Thomas cluster process [26]) with a scattering variance of σ_s^2 . SUs outside the clusters are the macro cell users. The locations of

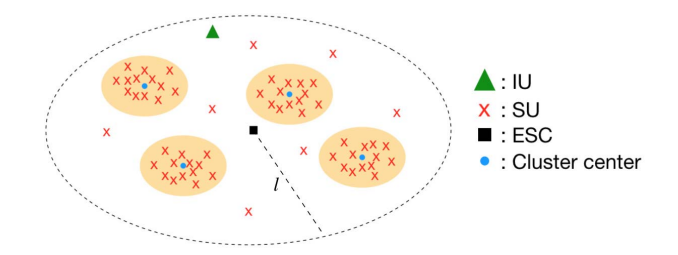


Fig. 2. Network of SUs and IUs in a two-tier user-centric deployed HetNets.

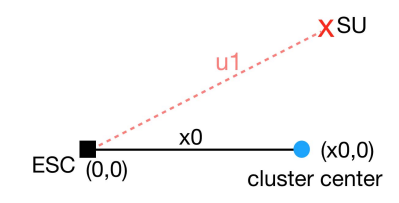


Fig. 3. The relation among hotspot SU, ESC and cluster center.

macro cell SUs are also modeled as a homogeneous PPP with the density of ρ_2 . ESC is denoted by a black square. Without loss of generality, we assume that each ESC is in charge of detecting the IU's presence in a large circular area centered at itself with a radius l. Thus, the average number of hotspot SUs in the given area is $\rho_1 n_s \pi l^2$, and the average number of macro cell SUs is $\rho_2 \pi l^2$.

B. Statistical Distribution of ESC e's Received SU Interference C_e

To derive the statistical distribution of C_e for ESC sensor e, the path attenuation between SU i and ESC e needs to be estimated. Since SU locations are usually not known to an ESC due to SU's location privacy protection, we cannot measure or compute the channel gain directly. Thus, we establish a statistical model of channel gain between SU and ESC. According to Section VII-A, the SUs are categorized into macro cell users and hotspot users. Thus, we model the distribution of distance between hotspot SU and ESC, denoted as u_1 , and the distribution of distance between macro cell SU and ESC denoted as u_2 , respectively. In this paper, we adopt the simplified path loss model $P^r(d) = P^t c d^{-\iota}$ for analysis since it captures the main characteristics of ray tracing. Here, $P^{r}(d)$ denotes the received power at distance d and P^{t} denotes the transmit power. c is a constant which is given by $c=\frac{P^r(\bar{d})\bar{d}^\iota}{P^t}$, \bar{d} is a reference distance, and ι is the path loss exponent. Hence, the channel gain between an ESC and a hotspot SU can be computed by $g_{u_1} = cu_1^{-\iota}$, and similarly $g_{u_2} = cu_2^{-\iota}$. Next, we examine the statistical distributions of u_1 and u_2 , which are used for modeling g_{u_1} and g_{u_1} .

1) Distribution of Distance u_1 Between Hotspot SU and ESC: We assume that the centers of SU clusters follow a homogeneous PPP, and hotspot SUs are normally distributed inside its cluster. The relation among hotspot SU, ESC and cluster center is illustrated in Figure 3, x_0 denotes the distance between cluster center and ESC.

According to [27], conditioned on the distribution of a cluster center, the distance u_1 from ESC to an SU follows the Rician distribution, and the conditioned probability density function (PDF) can be written as $\xi_{U_1|X}(u_1|x_0) = \frac{u_1}{\sigma_s^2} \exp(-\frac{u_1^2 + x_0^2}{2\sigma_s^2}) \cdot I_0(\frac{u_1 x_0}{\sigma_s^2})$. where $I_0(\cdot)$ is the modified Bessel function with order zero and σ_s^2 is the scattering variance. Since cluster centers are uniformly distributed, and the PDF is given by $\xi_X(x_0) = \frac{2x_0}{l^2}$. Thus, the PDF of u_1 can be computed based on $\xi_{U_1}(u_1) = \int_{x_0} \xi_{U_1|X}(u_1|x_0) \xi_X(x_0) \mathrm{d}x_0$.

- 2) Distribution of Distance u_2 Between Macro Cell SU and ESC: We assume that macro cell SUs are uniformly distributed inside the given area. The PDF of u_2 , denoted as $\xi(u_2)$, can be expressed as $\xi_{U_2}(u_2) = \frac{2u_2}{l^2}$.
- 3) Distribution of g_{u_1} , g_{u_2} and C_e : So far we have derived the PDFs for u_1 and u_2 , and the distributions of their corresponding channel gain g_{u_1} and g_{u_2} can be derived based on:

$$Pr(g_{u_1} \le g) = Pr(u_1 \ge (\frac{g}{c})^{-\frac{1}{\iota}}) = 1 - Pr(u_1 \le (\frac{g}{c})^{-\frac{1}{\iota}}),$$
(28)

$$\xi_{g_{u_1}}(g) = \frac{c^{\frac{1}{\iota}}}{\iota} g^{-\frac{1+\iota}{\iota}} \xi_{U_1}(c^{\frac{1}{\iota}} g^{-\frac{1}{\iota}})$$
(29)

Then the expectation \bar{g}_{u_1} and variance $\sigma^2_{g_{u_1}}$ of g_{u_1} can be derived from the PDF $\xi_{g_{u_1}}(g)$ of channel gain g_{u_1} . The PDF of g_{u_2} is derived in the same way, and the expectation and variance of g_{u_2} , denoted as \bar{g}_{u_2} and $\sigma^2_{g_{u_2}}$ can also be derived. Since all hotspot and macro cell SUs are independent,

Since all hotspot and macro cell SUs are independent, g_{u_1} is i.i.d. and g_{u_2} is also i.i.d.. C_e is then re-expressed as $C_e = \sum_{i=1}^{\rho_1 n_s \pi l^2} P_i^h g_{u_1} + \sum_{i=1}^{\rho_2 \pi l^2} P_i^m g_{u_2}$, where P_i^h and P_i^m denote the transmit power of hotspot SU and macro cell SU, respectively. Given the number of hotspot SUs $\rho_1 n_s \pi l^2$ and the number of macro cell SUs $\rho_2 \pi l^2$ in the model, when $\rho_1 n_s \pi l^2$ and $\rho_2 \pi l^2$ increase, using the Central Limit Theorem and the Law of Large Numbers, C_e can be approximated by a summation of two normal distributions which is still a normal distribution, $C_e \sim N(\mu_e, \sigma_e^2)$, where $\mu_e = \sum_{i=1}^{\rho_1 n_s \pi l^2} P_i^h \bar{g}_{u_1} + \sum_{i=1}^{\rho_2 \pi l^2} P_i^m \bar{g}_{u_2}, \sigma_e^2 = \sum_{i=1}^{\rho_1 n_s \pi l^2} (P_i^h)^2 \sigma_{g_{u_1}}^2 + \sum_{i=1}^{\rho_2 \pi l^2} (P_i^m)^2 \sigma_{g_{u_2}}^2$.

C. Statistical Distribution of IU's Received SU Interference I

In this section, we model the statistical distribution of the IU's received SU interference I. Denoting g_{v_1} as the path loss from a hotspot SU to the IU and g_{v_2} as the path loss from a macro cell SU to the IU, we again re-express I as $I = \sum_{i=1}^{\rho_1 n_s \pi l^2} P_i^h g_{v_1} + \sum_{i=1}^{\rho_2 \pi l^2} P_i^m g_{v_2}$. Same as C_e , to model I, we again need to derive g_{v_1} and g_{v_2} 's statistical distribution while IU's location is not explicitly known due to IU location privacy protection.

The first step for modeling g_{v_1} and g_{v_2} is to establish the statistical model of IU's location range to ESC, denoted as d_0 , given ESC's local measurement of IU signal strength. Then, based on this model, each ESC independently estimate d_0 , which leads to the derivation of g_{v_1} and g_{v_2} as well as the distribution of I and $U(T_E)$ in (27). It is important to note that this calculation process satisfies FCC's security regulation, which demands that ESCs must not share any IU's

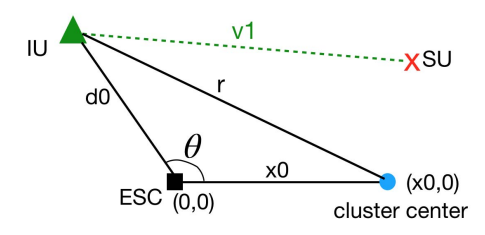


Fig. 4. The relation among IU, ESC, SU and cluster center.

location-related information. In our algorithm, ESC only uses local information and there is no exchange of any IU-related information with other ESC or other parties in the system.

- 1) Distribution of d_0 Based on ESC's local IU Signal Strength: We assume IU's transmit power P_{IU}^t is known since the general transmit power of 3.5GHz IU transmitters, such as radar systems, is easily found [28]. Hence, given the received IU signals, denoted as P_{IU}^r , an ESC can roughly model the distribution of its channel gain to IU as g_0 through a path loss formula $g_0 = P_{IU}^r/P_{IU}^t$. Thus, the distance between ESC and IU, denoted as d_0 , is given by $d_0 = \left(\frac{g_0}{c_0}\right)^{-\frac{1}{\iota}}$ where c_0 is a constant. Assuming IU's signal is transmitted through a Rayleigh fading channel, the CDF of P_{IU}^r can be modeled as $\Xi_{PR}(P_{IU}^r) = 1 \exp\left(-\frac{P_{IU}^r}{s_e}\right)$, where s_e is the expectation of P_{IU}^r , which can be measured by ESC e. Therefore, the CDF of g_0 is given by $\Xi_{G_0}(g_0) = 1 \exp\left(-\frac{g_0P_{IU}^r}{s_e}\right)$. The CDF of d_0 is then computed by $\Xi_{D_0}(d_0) = \exp\left(-\frac{c_0d_0^{-\iota}P_{IU}^t}{s_e}\right)$. Finally, the PDF of d_0 can be derived based on its CDF.
- 2) Distribution of Distance v_1 Between Hotspot SU and IU: The relation among IU, ESC, hotspot SU and cluster center is illustrated in Figure 4. From an ESC's perspective, IU's possible location is uniformly distributed on a circle that is centered at itself and has a radius of d_0 . We denote the distance from cluster center to IU as r, and the angle between d_0 and x_0 as θ .

To derive the distribution of v_1 , we need to compute the distribution for r. Clearly, r satisfies $r^2=d_0^2+x_0^2-2d_0x_0\cos\theta$. Since x_0,θ,d_0 are independent, and the PDF of θ is $\xi_\Theta(\theta)=\frac{1}{\pi}$, $\Xi_R(r)$ is derived as $\Xi_R(r)=\int_0^l \frac{2x_0}{l^2}\int_0^l \frac{1}{\pi}\arccos\frac{d_0^2+x_0^2-r^2}{2d_0x_0}\left[\exp(-\frac{c_0P_{IU}^td_0^{-\iota}}{s_e})\frac{\iota c_0P_{IU}^t}{s_e}d_0^{-\iota-1}\right]\mathrm{d}d_0\mathrm{d}x_0$, hence, r's PDF $\xi_R(r)$ can also be derived.

Having $\xi_R(r)$, the next step is to compute the PDF of v_1 . Similarly, conditioned on the distance r between an IU and a cluster center, the distance v_1 from IU to the SU, who is in a Thomas cluster process, is also Rician distributed, and the conditioned PDF is given by $\xi_{V_1|R}(v_1|r) = \frac{v_1}{\sigma_s^2} \exp(-\frac{v_1^2 + r^2}{2\sigma_s^2}) I_0(\frac{v_1 r}{\sigma_s^2})$. Then the PDF of v_1 can be derived by $\xi_{V_1}(v_1) = \int_r \xi_{V_1|R}(v_1|r) \xi_R(r) dr$.

3) Distribution of Distance v_2 Between Macro Cell SU and IU: From an ESC's perspective, once the value of d_0 is determined, the possible location of IU should be uniformly distributed in a circle that is centered at itself and has a radius of d_0 . Denote v_2 as the distance between a macro cell SU and IU. PDF of v_2 conditioned on d_0 , denoted as $\xi_{V_2|D_0}(v_2|d_0)$,

is expressed as:

$$\xi(v_2|d_0) = \begin{cases}
\frac{2v_2}{l^2}, & 0 \le v_2 \le l - d_0 \\
\frac{2v_2}{\pi l^2} \arccos(\frac{d_0^2 + v_2^2 - l^2}{2d_0 v_2}), & l - d_0 < v_2 \le l + d_0
\end{cases}$$
(30)

Thus v_2 's PDF can be computed based on $\xi_{V_2}(v_2) = \int_{d_0} \xi_{V_2|D_0}(v_2|d_0)\xi_{D_0}(d_0)\mathrm{d}d_0$.

4) Distribution of g_{v_1} , g_{v_2} and I: Given the derived the PDFs for distance v_1 and v_2 , the corresponding PDFs of channel gain g_{v_1} and g_{v_2} can be derived in the same way as in (28).

The expectation \bar{g}_{v_1} and variance $\sigma^2_{g_{v_1}}$ of g_{v_1} can be calculated based on the distribution of g_{v_1} . Similarly, g_{v_2} 's expectation \bar{g}_{v_2} and variance $\sigma^2_{g_{v_2}}$ can also be derived from g_{v_2} distribution.

Because all hotspot and macro cell SUs are independent, g_{v_1} is i.i.d. and g_{v_2} are also i.i.d.. When the number of hotspot SUs and the number of macro cell SUs increase, using the Central Limit Theorem and the Law of Large Numbers, $I = \sum_{i=1}^{\rho_1 n_s \pi l^2} P_i^h g_{v_1} + \sum_{i=1}^{\rho_2 \pi l^2} P_i^m g_{v_2}$ can be approximated by a normal distribution, $I \sim N(\mu_I, \sigma_I^2)$, where $\mu_I = \sum_{i=1}^{\rho_1 n_s \pi l^2} P_i^h \bar{g}_{v_1} + \sum_{i=1}^{\rho_2 \pi l^2} P_i^m \bar{g}_{v_2}, \sigma_I^2 = \sum_{i=1}^{\rho_1 n_s \pi l^2} (P_i^h)^2 \sigma_{g_{v_1}}^2 + \sum_{i=1}^{\rho_2 \pi l^2} (P_i^m)^2 \sigma_{g_{v_2}}^2$.

D. Determine ESCs' Interference Constraints

In Section VII-B and VII-C, we approximate C_e and I by normal distributions. The remaining problem to solve $U(\mathbf{T_E}) \geq \Psi$ in (27) is how each ESC e independently chooses a proper value of T_e . To achieve this, we rewrite (27) to:

$$U(\mathbf{T_E}) = Pr\left(\sum_{i=1}^{\rho_1 n_s \pi l^2} P_i^h g_{v_1} + \sum_{i=1}^{\rho_2 \pi l^2} P_i^m g_{v_2} \le T \right)$$

$$\times \sum_{i=1}^{\rho_1 n_s \pi l^2} P_i^h g_{u_1} + \sum_{i=1}^{\rho_2 \pi l^2} P_i^m g_{u_2} \le T_e,$$

$$\forall e \in [1, m_2] \ge \Psi. \tag{31}$$

Given that channel gains and transmit powers are all non-negative, and $I = \sum_{i=1}^{\rho_1 n_s \pi l^2} P_i^h g_{v_1} + \sum_{i=1}^{\rho_2 \pi l^2} P_i^m g_{v_2}$ and $C_e = \sum_{i=1}^{\rho_1 n_s \pi l^2} P_i^h g_{u_1} + \sum_{i=1}^{\rho_2 \pi l^2} P_i^m g_{u_2}$, we have $Pr(I \leq T | C_e \leq T_e, \text{for all } e) \geq Pr(I \leq T | C_e \leq T_e) \geq Pr(I \leq T | C_e = T_e)$. Thus, so long as each ESC sensor e independently computes a T_e that satisfies this inequality $Pr(I \leq T | C_e = T_e) \geq \Psi$, we know (27) must hold, meaning that IU's interference requirement is statistically guaranteed.

Based on the theory of conditional normal distribution [29], the conditional random variable $I|C_e=T_e$ is also normally distributed, with expectation μ_{Ie} and variance σ_{Ie} computed by:

$$\mu_{Ie} = \mu_I + \frac{\Sigma_{12}}{\Sigma_{22}} (T_e - \mu_e), \sigma_{Ie} = \Sigma_{11} - \frac{\Sigma_{12}^2}{\Sigma_{22}},$$
(32)

where
$$\Sigma_{11} = cov(I, I)$$
, $\Sigma_{12} = cov(I, C_e)$, (33)

$$\Sigma_{22} = cov(C_e, C_e), \tag{34}$$

where function $cov(\cdot)$ calculates the covariance of the two input distributions. Since the distribution of $I|C_e=T_e$ is known, given a Ψ , the value of μ_{Ie} , denoted as μ_0 , that makes $Pr(I \leq T|C_e=T_e) \geq \Psi$ can be computed as $\mu_0=T_e-\sigma_{Ie}\Phi^{-1}(\Psi)$. Here, $\Phi^{-1}(\cdot)$ is the quantile function of standard normal distribution. Thus, based on (32), T_e can be calculated by

$$T_e = (\mu_0 - \mu_I) \frac{\Sigma_{22}}{\Sigma_{12}} + \mu_e.$$
 (35)

(35) is the formula used by each ESC e to generate T_e locally as its interference requirement. With a proper T_e in the algorithm (6), the IU's interference requirement is statistically guaranteed.

E. Multiple IU Cases

So far only the scenario with one IU is considered. However, the way to handle multiple IUs in ESC requirement computation is straightforward. If an ESC e detects the existence of multiple IUs, it can simply compute the constraint threshold for each IU and choose the minimum one as final T_e , such that (27) is guaranteed for every IU. Note that there are a large amount of existing focusing on wireless signal classification, including traditional signal classification [21], [30] and deep learning based classification [23], [31], [32]. The ESCs can distinguish multiple IU signals by adopting some of these signal classification approaches.

VIII. ANALYSIS ON IU LOCATION PROTECTION

In this section, we demonstrate how the IU's location privacy is protected in our algorithm. As seen from our algorithm, since ESCs are responsible for detecting an IU's existence in the spectrum and measuring the average received IU signal strength. ESCs are the only entities that obtain information directly related to the IU's location. In our attack model, we assume ESCs are trustworthy so an adversary cannot know its raw measurement of IU RSS. But the adversary may see all the information exchanged in the DSA system by compromising SAS, BSs, SUs or the communication channel. The attacker will attempt to derive sensitive IU location data from information that they observed.

According to (6) - (11) and Section VII, each ESC e uses the average IU signal strength s_e to generate its requirement T_e and computes Δ_e to be sent to SAS. The minimum value Δ of Δ_e s is then forwarded to SUs. From the adversary's perspective, since Δ 's and Δ_e 's computation are both based on T_e , which again relates to the distance between IU and ESC e, Δ_e and Δ may carry some IU location information and can be used to infer the changes in IU's true location.

In this section, we mainly focus on the case with one IU to analyze the strength of Δ_e on IU location protection. If the attacker cannot infer IU location changes from Δ_e s in this simple case, neither can he derive the IU location changes from Δ or in multiple IU cases. This is because Δ

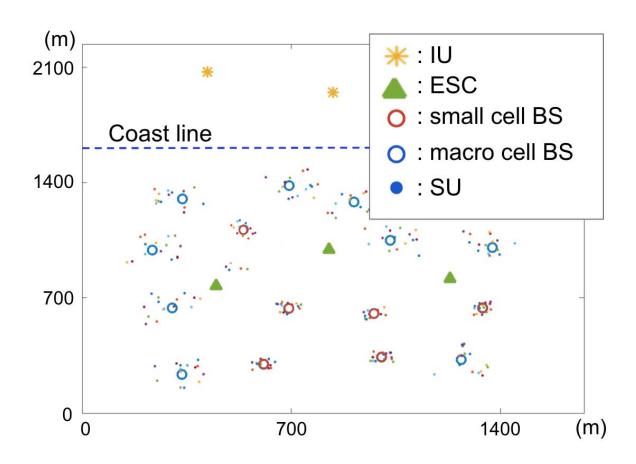


Fig. 5. Example of our simulation settings.

is the minimum value of $\Delta_e, e \in [1, m_2]$. Thus, it contains no additional information regarding IU locations comparing to Δ_e s. In multiple IU cases, Δ_e s calculated by ESC e in different iterations may not match to the same IU. Thus, Δ_e in this case may not have the consecutive location information of any IU, which makes deriving a single IU location change even harder comparing to a single IU case.

Consider a single IU case. To ensure that IU-ESC distance changes cannot be discovered in a sequence of Δ_e , our method increases the randomness in the value of Δ_e by using random numbers η_1 and η_2 in the generation of Δ_e as shown in equation (6). To analyze if the variations in Δ_e are related with the changes in IU's location, one can calculate the correlation and p-value between the sequence of Δ_e and the IU-ESC distances [33]. Correlation coefficient and p-value are often used together to measure the strength of the relationship between two variables. A lower p-value can be interpreted as a stronger relation between two sets of data, and a p-value higher than 0.05 means that the correlation is not statistically significant [33]. If the sequences of Δ_e and IU-ESC distances have a low correlation coefficient with a large p-value, we can say that the correlation between Δ_e s and IU-ESC distances is not statistically significant, and the attacker can hardly use Δ_e s to infer the IU's true location. Using this method, in evaluation section IX-C, we compute the correlation coefficient and p-value through simulation.

IX. EVALUATION

In this section, we evaluate the performance of the proposed uplink power control algorithm by simulation. The simulation platform is MATLAB 2018a on a macOS Sierra with 2.7 GHz Intel Core i5 processor. Evaluation for the proposed algorithm is divided into two sets. The first set considers the scenario with static SUs and IUs, and the second set assumes the mobility of SUs and IUs. Both sets examine the secondary network utility, convergence speed of SU transmit power, SINR of SUs and the SU interference received at IU.

Figure 5 shows an example of our simulation setting. We consider spectrum sharing in the 3.5 GHz band which is implemented mainly along the U.S. coastal areas. SUs, BSs and

TABLE II
PARAMETER SETTINGS

Parameter	Description	Value
ρ_1	Density of cluster centers	$5 \times 10^{-6}/m^2$
$ ho_2$	Density of macro cell SUs	$1 \times 10^{-5}/m^2$
n_s	Avg. No. of hotspot SUs	15
σ_s	Scattering variance	40m
l	ESC sensing range	1000m
P_{IU}^t	IU's transmit power	1000W

TABLE III
AVERAGE CONVERGENCE SPEED OF SU'S TRANSMIT POWER

SU number	60	135	240
Avg. iterations for convergence	139.2122	146.0846	151.3658

ESCs are located inland and the IUs are randomly distributed in the sea. Both IUs and SUs can be mobile, and cases with different IUs' and SUs' speeds are evaluated in the second set of the simulation. In terms of parameter settings, the number of macro cell BS is set to $\{2, 5, 10\}$, the number of small cell BS is set to $\{2,4,6\}$, the number of SUs communicating with each BS is 15, and the ESC number is chosen from 2 to 4. The range of SU's minimum required SINR τ is selected from 30 to 100, and IU's maximum allowable interference T is set to $\{10^{-7}, 10^{-6}, 10^{-5}\}W$. Each ESC senses the interference from both SUs and IU 100 times per second. Each BS broadcasts the required information per 10 millisecond. We assume that in our algorithm the messages transmitted between entities are all 16-bit floating point numbers. By using time series compression with delta encoding [34], [35], the data transmission rate of each BS to its SUs is around 7 Mbps. Each SU reads its location information at a rate of 10Hz from a GPS sensor. A standard path loss model is applied for each SU. The path loss exponent ι is set to 4. The maximum SU transmit power is 1W. The environment interference φ_i to BS i includes both the receiver noise and other environment noises, and is set to -80dbm. Parameters used by ESC to theoretically estimate its interference threshold are shown in Table II.

A. Stability Analysis

1) Case With Static IU and SU: In the first set of simulation, we examine the algorithm's performance given static IU and SU. Table III shows the average convergence speed of SU's transmit power. In this case, $\tau=50$, $T=10^{-6}W$, numESC=3. The system is assumed to be stable when the fluctuations in transmit power are smaller than 0.0001W. It can be observed that SU's transmit power converges quickly in less than 200 iterations. Only a slight increase in the convergence speed is observed as the total number of SU increases, which indicates the good scalability of our algorithm.

Next, we evaluate our algorithm's performance in achieving the maximum network utility (sum of SU rates). We randomly generate 100 simulation settings for the comparison between our algorithm and the Global Search algorithm [36]. Global Search uses a multi-start framework designed to find global optima for pure and mixed integer nonlinear problems with

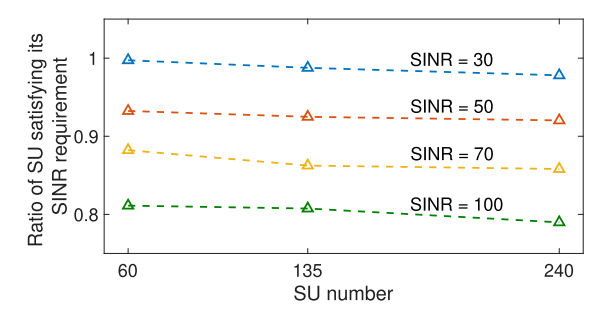


Fig. 6. Ratio of SU satisfying its SINR requirement.

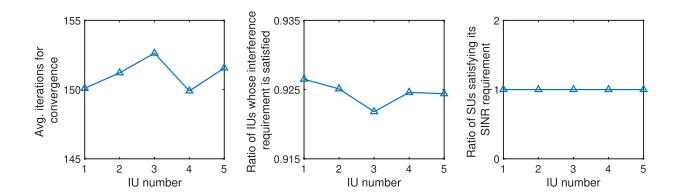


Fig. 7. Our algorithm's performance under different IU number.

many constraints and variables. By processing all the results, we observe that our algorithm outperforms Global Search in every test given SU number equal to 60 and 135, and when SU number equal to 240, our algorithm outperforms Global Search in 99% of the tests. As mentioned, DCA converges quite often to a global solution in practice, this comparison at least demonstrates that our algorithm performs better than a commonly used global solver in finding the global optima of the given uplink power control problem. Moreover, for each setting, the average running time of our algorithm for convergence is around 3.5 seconds, and it is much smaller than the running time of the Global Search algorithm which is around 70.5 seconds.

Figure 6 shows the average ratio of SU satisfying its SINR requirement given different SUs numbers and SU SINR requirements. We can see that the amount of SUs who have their SINR guaranteed is gradually decreasing as the minimum required SINR grows. This is intuitive since it becomes harder to meet every SU's required SINR when all SUs are demanding for higher SINR. However, given a certain SINR, there is only a slight decrease in the percentage as the total SU number increases, which also indicates the good scalability of our algorithm.

Next, we calculate the ratio of IU satisfying its interference requirement under different parameter settings, where the number of SU ranges from 60 to 240, the number of ESC ranges from 2 to 4 and the IU's interference requirement is set to $\{10^{-7}W, 10^{-6}W, 10^{-5}W\}$. We observe from the results that the interference received by IU is guaranteed 100% of time to be below their requirements under all the above settings.

We also evaluate the effect of the number of IU on system performance as shown in Figure 7. In this simulation, we set $SUnum=240,\ ESCnum=3,\ \tau=50$ and $T=10^{-6}W.$ Given IU number from 1 to 5, we evaluated the average convergence speed of SU's transmit power, the ratio of SUs whose required SINR is satisfied and the ratio of IUs whose interference requirement is met. As in Figure 7, both the

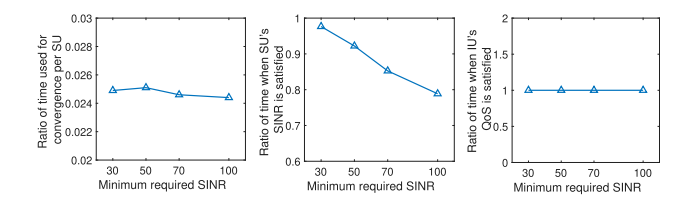


Fig. 8. Our algorithm's performance under different minimum required SINR.

average iterations SU uses for convergence and the ratio of SUs satisfying its require SINR are not obviously influenced by different IU numbers. It is because when an ESC e detects the existence of multiple IUs, it can simply compute the constraint threshold for each IU and choose the minimum one as final T_e , and the following SU power update procedure is the same as that in one IU case. Different T_e s only affect the upper bound on SU's power adaptation step size. We also observe from the results that the interference received by all IUs is always guaranteed to be below their requirements under all the above settings.

2) Case With Mobile IU and SU: The second set of simulations takes the mobility of IU and SU into consideration. Each simulation lasts for 10 minutes (i.e. 60000 iterations). In the simulation, both ESC and BS broadcast their information per 10 ms, and SU updates its location information 10 times per second. The number of macro cell BS is set to 10 and the number of small cell BS's is 6. ESC number is set to 3 in this case.

We first set IU's moving speed to 10m/s and SU's moving speed to 1m/s. In Figure 8, it can be seen that each SU only takes around 2% of its total operation time in the convergence process. We also observe that the average amount of time during which the SU's SINR is satisfied is gradually decreasing as the minimum required SINR grows, since it becomes more difficult to guarantee the SUs' target SINR if they are requiring for higher SINR. However, IU's interference requirement is satisfied 100% of time, because our algorithm treats IU's interference constraint with higher priority than SU's SINR requirement. By using this algorithm, IU's interference requirement is statistically guaranteed by ESC's interference threshold in any case even when SUs' and IUs' constraints cannot be satisfied simultaneously (i.e. $\widetilde{S} = \emptyset$).

Figure 9 shows our algorithm's convergence under different IU's and SU's moving speeds. In this case, the required SU SINR is set to 50. In the left figure of Figure 9, SU's moving speed is set to 1m/s and IU's speed varies from 1m/s to 30m/s. Because the IUs in 3.5 GHz DSA scenario are commonly shipborne radars, the simulation settings of IU's speed are determined based on the speed range of navy ships which is mostly less than $30 \ m/s$. In addition, such parameter settings also satisfy the speed range of some other vehicles like cars, hence the IUs in our simulation are not necessarily specified as shipborne radars. We can see that the system's convergence time is not obviously influenced by the changes in IU's speed, because IU's location only affects the calculation of ESC's interference requirement which only provides an upper bound on SU's power adaptation step size.

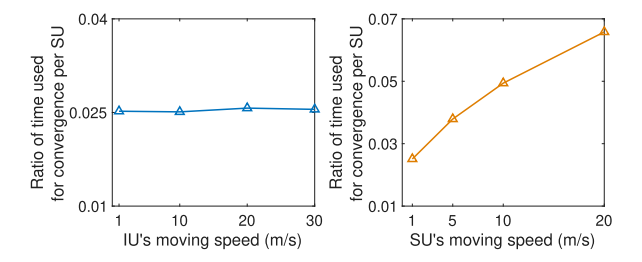


Fig. 9. Left figure shows the ratio of time used for convergence per SU given different IU's moving speed. Right figure shows the ratio of time used for convergence per SU given different SU's moving speed.

In the right figure of Figure 9, IU's moving speed is fixed to 10m/s and SU's moving speed ranges from 1m/s to 20m/s (e.g., from walking speed to freeway speed). It can be seen that the average convergence time per SU slightly increases as the SU's moving speed increases. It is intuitive because when an SU's speed increases, its movement within an iteration becomes larger and it becomes harder to converge. However, the observed increase is relatively small, which means our algorithm is not very sensitive to the SU's moving speed. By processing all the results, we also observe that IU's interference requirement is always guaranteed under different moving speeds of both SUs and IUs.

B. Efficiency Evaluation

First, we compare our algorithm with the existing primary user (PU) protection schemes [37], [38] in terms of network throughput under the same IU interference protection level. A geographic exclusion zone (GEZ) scheme in [37] calculates the minimum radius of the primary exclusion zone based on the primary outage constraint, and [38] proposes a shapeless PU protection scheme called the discrete exclusion zone (DEZ), which is achieved by switching off the first k-1 nearest neighboring SUs surrounding the PU. With IU's interference requirement equal to $10^{-8}W$ and the number of SUs equal to 240, the minimum radius of exclusion zone in GEZ ends up to be 1000m and the number of SUs being switched off in DEZ becomes 70. Under these settings, our scheme can improve total SU capacity by 56% over GEZ and by 48% over DEZ on average.

We also compare our algorithm with three power control algorithms all aiming at throughput maximization subject to satisfying a minimum target SINR for all SUs. [10] developed an efficient centralized DC algorithm that achieves the global optimal throughput. A binary power control algorithm is proposed in [39] to maximize the total SU throughput in a CRN while limiting the interference to the PU within an acceptable range. [40] proposed a distributed algorithm aiming at maximizing the throughput with minimum power consumption.

In the evaluation, we assume 9 to 36 pairs of SU transmitters/receivers are distributed in a $500m \times 500m$ square. Because the formulation of [10] and [40] do not consider PU (IU) interference constraint, we assume the PU locates far enough from SU network, and hence the PU will not be affected by SUs, the PU interference requirement in our

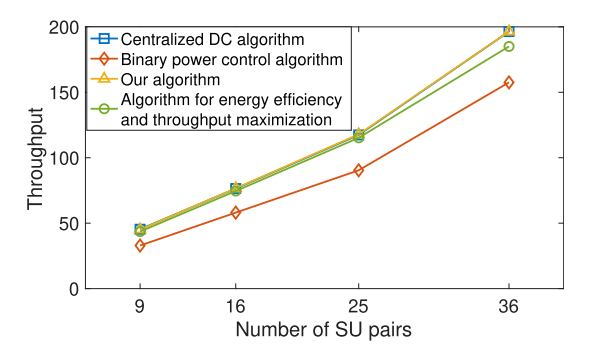


Fig. 10. Comparison between our algorithm and three power control algorithms on throughput.

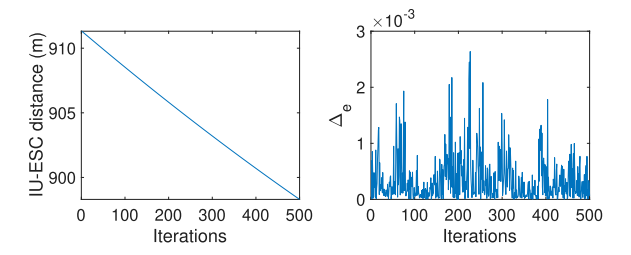


Fig. 11. Left figure shows 500 iterations of one sequence of IU-ESC distances and right figure shows the corresponding Δ_e s.

algorithm and [39] will not be violated even when all SUs transmit at the maximum power simultaneously. 100 simulation settings are randomly generated for each number of SU pair. The average throughput of each algorithm is measured. From Figure 10, we can see that our algorithm outperforms binary algorithm [39] and the algorithm for energy efficiency and throughput maximization [40]. The average throughput achieved by our algorithm and centralized DC algorithm [10] are almost the same. This is because our algorithm and [10] both refer to Frank and Wolfe feasible direction algorithm [41] to locate the global optimal solution to the formulated nonconvex problem.

C. Evaluation on IU Location Protection

In the evaluation, we randomly generate 500 settings of locations of a moving IU, 3 ESCs and 240 static SUs. Each simulation with one setting lasts for 60000 iterations. Figure 11 zooms in for the 500 iterations of example sequences of IU-ESC distances and Δ_e s. The average correlation coefficient between the sequences of IU-ESC distances and Δ_e s is around 0.07 which can be considered negligible [42], and the p-value is around 0.31 which is much larger than 0.05 [33]. Hence, we can conclude that the correlation is not statically significant. Such low correlation indicates that it is difficult for an attacker to infer IU's true location from Δ_e s.

X. CONCLUSION

In this paper, we studied the uplink power control problem in 3.5 GHz DSA systems with the objective of utility maximization subject to SU's transmit power limit and SINR constraints and IU's interference constraints. Due to security considerations, the proposed distributed SU transmit power control algorithm does not depend on any sensitive information from IU. IU's interference requirement is proved to be guaranteed by our algorithm in any case. Each SU only requires locally observable measurements with aggregated insensitive information provided by ESCs and BSs to adjust its transmit power distributively. Through the analysis on the algorithm's convergence and stability properties, we demonstrate that our algorithm will converge to a stable optimal point which always satisfies the IU's interference constraint. SUs' SINR requirements will also be satisfied whenever the utility maximization problem is feasible. Finally, the simulation results demonstrate the effectiveness of our proposed algorithm.

REFERENCES

- [1] G. Locke and L. E. Strickling, "Plan and timetable to make available 500 megahertz of spectrum for wireless broadband," U.S. Dept. Commerce, Washington, DC, USA, President's Spectrum Plan Rep., 2010. [Online]. Available: https://www.ntia.doc.gov/report/2010/ten-yearplan-and-timetable-make-available-500-megahertz-spectrum-wirelessbroadband-pre
- [2] P. Kolodzy and I. Avoidance, "Spectrum policy task force," Federal Commun. Commun., Washington, DC, USA, ET Docket Rep. 02-135, 2002, pp. 147–158, vol. 40, no. 4.
- [3] Y. Lin, Y. Ye, and Y. Yang, "Preserving incumbent user's location privacy against environmental sensing capability," in *Proc. IEEE Int. Symp. Dyn. Spectr. Access Netw. (DySPAN)*, Nov. 2019, pp. 1–10.
- [4] H.-S.-T. Le and Q. Liang, "An efficient power control scheme for cognitive radios," in *Proc. IEEE Wireless Commun. Netw. Conf.*, Mar. 2007, pp. 2559–2563.
- [5] W. Wang, T. Peng, and W. Wang, "Optimal power control under interference temperature constraints in cognitive radio network," in *Proc. IEEE Wireless Commun. Netw. Conf.*, Mar. 2007, pp. 116–120.
- [6] L. P. Qian, S. Zhang, W. Zhang, and Y. J. Zhang, "System utility maximization with interference processing for cognitive radio networks," *IEEE Trans. Commun.*, vol. 63, no. 5, pp. 1567–1579, May 2015.
- [7] X. Li, J. Fang, W. Cheng, H. Duan, Z. Chen, and H. Li, "Intelligent power control for spectrum sharing in cognitive radios: A deep reinforcement learning approach," *IEEE Access*, vol. 6, pp. 25463–25473, 2018.
- [8] L. Zheng and C. W. Tan, "Cognitive radio network duality and algorithms for utility maximization," *IEEE J. Sel. Areas Commun.*, vol. 31, no. 3, pp. 500–513, Mar. 2013.
- [9] C. W. Tan, "Optimal power control in Rayleigh-fading heterogeneous wireless networks," *IEEE/ACM Trans. Netw.*, vol. 24, no. 2, pp. 940–953, Apr. 2016.
- [10] H. H. Kha, H. D. Tuan, and H. H. Nguyen, "Fast global optimal power allocation in wireless networks by local D.C. programming," *IEEE Trans. Wireless Commun.*, vol. 11, no. 2, pp. 510–515, Feb. 2011.
- [11] L. Zheng and C. W. Tan, "Maximizing sum rates in cognitive radio networks: Convex relaxation and global optimization algorithms," *IEEE J. Sel. Areas Commun.*, vol. 32, no. 3, pp. 667–680, Mar. 2014.
- [12] B. Gedik and L. Liu, "Protecting location privacy with personalized k-anonymity: Architecture and algorithms," *IEEE Trans. Mobile Comput.*, vol. 7, no. 1, pp. 1–18, Jan. 2008.
- [13] B. Bahrak, S. Bhattarai, A. Ullah, J.-M.-J. Park, J. Reed, and D. Gurney, "Protecting the primary users' operational privacy in spectrum sharing," in *Proc. IEEE Int. Symp. Dyn. Spectr. Access Netw. (DYSPAN)*, Apr. 2014, pp. 236–247.
- [14] M. Clark and K. Psounis, "Can the privacy of primary networks in shared spectrum be protected?" in *Proc. 35th Annu. IEEE Int. Conf. Comput. Commun. (IEEE INFOCOM)*, Apr. 2016, pp. 1–9.
- [15] Q. Cheng, D. N. Nguyen, E. Dutkiewicz, and M. D. Mueck, "Protecting operational information of incumbent and secondary users in FCC spectrum access system," in *Proc. IEEE Int. Conf. Commun. (ICC)*, May 2018, pp. 1–6.
- [16] H. Li, Y. Yang, Y. Dou, J.-M.-J. Park, and K. Ren, "PeDSS: Privacy enhanced and database-driven dynamic spectrum sharing," in *Proc. IEEE Conf. Comput. Commun. (IEEE INFOCOM)*, Apr. 2019, pp. 1477–1485.
- [17] H. Li, Y. Dou, C. Lu, D. Zabransky, Y. Yang, and J.-M.-J. Park, "Preserving the incumbent users' location privacy in the 3.5 GHz band," in *Proc. IEEE Int. Symp. Dyn. Spectr. Access Netw. (DySPAN)*, Oct. 2018, pp. 1–10.

- [18] Wireless Telecommunications Bureau and Office of Engineering and Technology Establish Procedure for Registering Environmental Sensing Capability Sensors, Federal Commun. Commission, FCC Public Notice, Washington, DC, USA, 2018.
- [19] N. Gulpinar, L. T. H. An, and M. Moeini, "Robust investment strategies with discrete asset choice constraints using DC programming," *Optimization*, vol. 59, no. 1, pp. 45–62, Jan. 2010.
- [20] L. T. Hoai An, "An efficient algorithm for globally minimizing a quadratic function under convex quadratic constraints," *Math. Program.*, vol. 87, no. 3, pp. 401–426, May 2000.
- [21] O. A. Dobre, A. Abdi, Y. Bar-Ness, and W. Su, "Survey of automatic modulation classification techniques: Classical approaches and new trends," *IET Commun.*, vol. 1, no. 2, pp. 137–156, Apr. 2007.
- [22] T. J. O'Shea, J. Corgan, and T. C. Clancy, "Convolutional radio modulation recognition networks," in *Proc. Int. Conf. Eng. Appl. Neural Netw.* Aberdeen, U.K.: Springer, 2016, pp. 213–226.
- [23] Y. Shi, K. Davaslioglu, Y. E. Sagduyu, W. C. Headley, M. Fowler, and G. Green, "Deep learning for RF signal classification in unknown and dynamic spectrum environments," in *Proc. IEEE Int. Symp. Dyn. Spectr.* Access Netw. (DySPAN), Nov. 2019, pp. 1–10.
- [24] S. Haile, "Investigation of channel reciprocity for OFDM TDD systems," M.S. thesis, Univ. Waterloo, ON. Canada, 2009.
- M.S. thesis, Univ. Waterloo, Waterloo, ON, Canada, 2009.
 [25] N. W. Anderson, "Uplink resource allocation to control intercell interference in a wireless communication system," U.S. Patent 8023 955, Sep. 20, 2011.
- [26] R. K. Ganti and M. Haenggi, "Interference and outage in clustered wireless ad hoc networks," *IEEE Trans. Inf. Theory*, vol. 55, no. 9, pp. 4067–4086, Sep. 2009.
- [27] M. Afshang and H. S. Dhillon, "Poisson cluster process based analysis of HetNets with correlated user and base station locations," *IEEE Trans. Wireless Commun.*, vol. 17, no. 4, pp. 2417–2431, Apr. 2018.
- [28] P. Hale, J. Jargon, P. Jeavons, M. Souryal, A. Wunderlich, and M. Lofquist, "3.5 GHz radar waveform capture at point LOMA," Nat. Inst. Standards Technol., Gaithersburg, MA, USA, Tech. Note NIST TN 1954, 2017. Accessed: Jun. 26, 2022. [Online]. Available: https://doi.org/10.6028/NIST.TN.1954
- [29] J. K. Patel and C. B. Read, Handbook of the Normal Distribution, vol. 150. Boca Raton, FL, USA: CRC Press, 1996.
- [30] W. C. Headley and C. R. C. M. D. Silva, "Asynchronous classification of digital amplitude-phase modulated signals in flat-fading channels," *IEEE Trans. Commun.*, vol. 59, no. 1, pp. 7–12, Jan. 2011.
- [31] M. Zheleva, R. Chandra, A. Chowdhery, A. Kapoor, and P. Garnett, "TxMiner: Identifying transmitters in real-world spectrum measurements," in *Proc. IEEE Int. Symp. Dyn. Spectr. Access Netw. (DySPAN)*, Sep. 2015, pp. 94–105.
 [32] M. Kulin, T. Kazaz, I. Moerman, and E. De Poorter, "End-to-end
- [32] M. Kulin, T. Kazaz, I. Moerman, and E. De Poorter, "End-to-end learning from spectrum data: A deep learning approach for wireless signal identification in spectrum monitoring applications," *IEEE Access*, vol. 6, pp. 18484–18501, 2018.
- [33] H. J. Hung, R. T. O'Neill, P. Bauer, and K. Kohne, "The behavior of the P-value when the alternative hypothesis is true," *Biometrics*, vol. 53, no. 1, pp. 11–22, 1997.
- [34] T. Pelkonen et al., "Gorilla: A fast, scalable, in-memory time series database," Proc. VLDB Endowment, vol. 8, no. 12, pp. 1816–1827, 2015.
- [35] J. C. Mogul, F. Douglis, A. Feldmann, and B. Krishnamurthy, "Potential benefits of delta encoding and data compression for. [Online]. Available: http," in *Proc. ACM SIGCOMM'97 Conf. Appl., Technol., architectures,* protocols for Comput. Commun., 1997, pp. 181–194.
- [36] Z. Ugray, L. Lasdon, J. Plummer, F. Glover, J. Kelly, and R. Martí, "Scatter search and local NLP solvers: A multistart framework for global optimization," *INFORMS J. Comput.*, vol. 19, no. 3, pp. 328–340, 2007.
- [37] U. Tefek and T. J. Lim, "Interference management through exclusion zones in two-tier cognitive networks," *IEEE Trans. Wireless Commun.*, vol. 15, no. 3, pp. 2292–2302, Mar. 2016.
- [38] C. Sun and R. Jiao, "Discrete exclusion zone for dynamic spectrum access wireless networks," *IEEE Access*, vol. 8, pp. 49551–49561, 2020.
- [39] D. Nakhale and M. Z. A. Khan, "Fast binary power allocation for uplink distributed cognitive radio networks," in *Proc. 10th Int. Conf. Commun.* Syst. Netw. (COMSNETS), Jan. 2018, pp. 435–438.
- [40] R. Aslani and M. Rasti, "A distributed power control algorithm for energy efficiency maximization in wireless cellular networks," *IEEE Wireless Commun. Lett.*, vol. 9, no. 11, pp. 1975–1979, Nov. 2020.
- [41] P. Apkarian and H. D. Tuan, "Robust control via concave minimization local and global algorithms," *IEEE Trans. Autom. Control*, vol. 45, no. 2, pp. 299–305, Feb. 2000.
- [42] D. E. Hinkle, W. Wiersma, and S. G. Jurs, *Applied Statistics for the Behavioral Sciences*, vol. 663. Boston, MA, USA: Houghton Mifflin College Division, 2003.



Yousi Lin received the B.S. degree in communication engineering from Shandong University, Shandong, China, in 2016, and the Ph.D. degree from the Department of Electrical and Computer Engineering, Virginia Tech, USA, in 2021. Her current research interests include resource allocation and scheduling, network optimization, joint design of communication and control in dynamic spectrum access systems, and 802.11 MAC protocol design.



Xiaojiang (James) Du (Fellow, IEEE) received the B.S. degree from Tsinghua University, Beijing, China, in 1996, and the M.S. and Ph.D. degrees in electrical engineering from the University of Maryland, College Park, in 2002 and 2003, respectively. He was a tenured Professor at Temple University from August 2009 to August 2021. He is currently the Anson Wood Burchard Endowed-Chair Professor at the Department of Electrical and Computer Engineering, Stevens Institute of Technology. His research interests are security, wireless networks,

and systems. He has authored over 500 journal and conference papers in these areas, including the top security conferences IEEE S&P, USENIX Security, and NDSS. He has been awarded more than eight million U.S. dollars research grants from the U.S. National Science Foundation (NSF), the Army Research Office, the Air Force Research Laboratory, the State of Pennsylvania, and Amazon. He is an ACM Distinguished Member and an ACM Life Member. He won the Best Paper Award at several conferences, such as IEEE ICC 2020 and IEEE GLOBECOM 2014, and the Best Poster Runner-Up Award at the ACM MobiHoc 2014. He serves on the editorial boards of three IEEE journals.



Yaling Yang (Member, IEEE) received the Ph.D. degree from the University of Illinois Urbana-Champaign. She was named the Faculty Fellow of the College of Engineering, Virginia Tech, in 2016, where she is currently a Full Professor with the Electrical and Computer Engineering Department. She has been the Principle Investigator of ten NSF projects and one National Security Agency project. She has close to 20 years of experiences on wireless network protocol design, the IoT platform design, and network security. She has more than 70 publi-

cations in these areas. For the IoT research, she has developed a novel IoT hardware platform and its accompanied development environment to support flexible hardware-software. On security aspect, she is currently leading three NSF projects studying the location security of dynamic spectrum access systems and smartphone-based contact tracing systems and has published in top security journals and conferences six works for her research in this aspect. Her work about GPS spoofing's threat towards vehicle navigation system has been reported world-wide by more than 30 news agencies. She has also published more than 20 papers regarding QoS guarantees in wireless networks. She is an NSF Career Award Winner. She won the Best Paper Award in SECON 2011 for her development of an innovative IoT simulator that can accurately capture the timing and energy consumptions of various platforms to hardware cycle level.



Jie Wu (Fellow, IEEE) has served as the Chair for the Department of Computer and Information Sciences from Summer 2009 to Summer 2016 and an Associate Vice Provost for international affairs from Fall 2015 to Summer 2017. He is currently the Director of the Center for Networked Computing and Laura H. Carnell Professor, Temple University. He also works as the Director of international affairs at the College of Science and Technology. Prior to joining Temple University, he was the Program Director at the National Science Foundation and a

Distinguished Professor at Florida Atlantic University. He regularly publishes in scholarly journals, conference proceedings, and books. His current research interests include mobile computing and wireless networks, routing protocols, network trust and security, distributed algorithms, applied machine learning, and cloud computing. He is a fellow of AAAS. He was a recipient of the 2011 China Computer Federation (CCF) Overseas Outstanding Achievement Award. He is/was the General Chair/Co-Chair for IEEE IPDPS'08, IEEE DCOSS'09, IEEE ICDCS'13, ACM MobiHoc'14, ICPP'16, IEEE CNS'16, WiOpt'21, and ICDCN'22, as well as the Program Chair/Co-Chair for IEEE MASS'04, IEEE INFOCOM'11, CCF CNCC'13, and ICCCN'20. He was an IEEE Computer Society Distinguished Visitor, an ACM Distinguished Speaker, and the Chair for the IEEE Technical Committee on Distributed Processing (TCDP). He serves on several editorial boards, including IEEE TRANSACTIONS ON MOBILE COMPUTING, IEEE TRANSACTIONS ON SER-VICES COMPUTING, Journal of Parallel and Distributed Computing, and Journal of Computer Science and Technology.